Supplementary Information

Curtailing FGF19's Mitogenicity by Suppressing its Receptor Dimerization Ability

Jianlou Niu[1,#], Jing Zhao[1,2,#], Jiamin Wu[1,#], Guanting Qiao[1], Junlian Gu[3], Chuanren Zhou[1], Qi Li[1], Lei Ying [4], Dezhong Wang[5], Huan Lin[1], Xiaokun Li[1], Zhifeng Huang[1,*], Moosa Mohammadi[6,*]

[1]School of Pharmaceutical Science, Wenzhou Medical University, Wenzhou, Zhejiang 325035, China.
[2]Department of Pharmacy, Zhejiang Hospital, Hangzhou, Zhejiang 310030, China
[3]School of Nursing, Shandong University, Jinan, Shandong 250100, China.
[4]School of Basic Medical Sciences, Wenzhou Medical University, Wenzhou, Zhejiang 325035, China.
[5]School of Life and Environmental Science, Wenzhou University, Wenzhou, Zhejiang, 325035, China.
[6]Department of Biochemistry & Molecular Pharmacology, School of Medicine, New York University, New York, NY 10016, United States.

[#]These authors contributed equally to this work.
*To whom correspondence should be addressed:
Email: hzf@wmu.edu.cn (Huang ZF) or moosa.mohammadi@nyumc.org (Mohammadi M)

www.pnas.org/cgi/doi/10.1073/pnas.2010984117

Figure S1

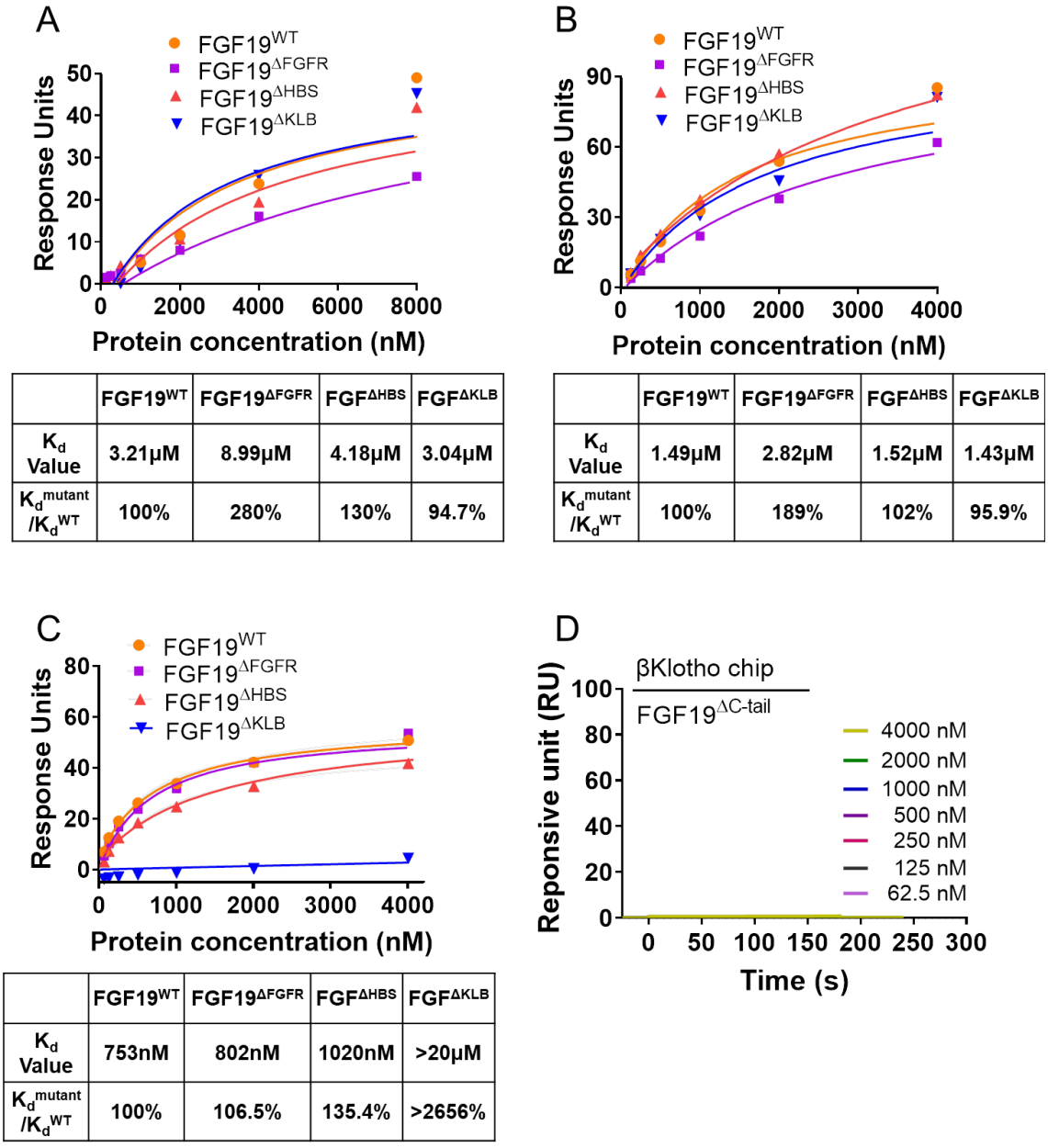

	FGF19^{WT}	FGF19$^{\Delta FGFR}$	FGF$^{\Delta HBS}$	FGF$^{\Delta KLB}$
K_d Value	3.21μM	8.99μM	4.18μM	3.04μM
K_d^{mutant}/K_d^{WT}	100%	280%	130%	94.7%

	FGF19^{WT}	FGF19$^{\Delta FGFR}$	FGF$^{\Delta HBS}$	FGF$^{\Delta KLB}$
K_d Value	1.49μM	2.82μM	1.52μM	1.43μM
K_d^{mutant}/K_d^{WT}	100%	189%	102%	95.9%

	FGF19^{WT}	FGF19$^{\Delta FGFR}$	FGF$^{\Delta HBS}$	FGF$^{\Delta KLB}$
K_d Value	753nM	802nM	1020nM	>20μM
K_d^{mutant}/K_d^{WT}	100%	106.5%	135.4%	>2656%

Figure S1. Binding affinities of FGF19^{WT} and its variants to FGFR4, FGFR1 and βKlotho (KLB). **(A-C)** Equilibrium binding responses obtained by passing increasing concentrations of FGF19^{WT} or its variants over sensor chips containing FGFR4 (A), FGFR1c (B) or KLB (C) were plotted as a function of analyte (FGF19^{WT} and its variants) concentration. Equilibrium dissociation constants (K_d values)

were derived from saturation binding curves (upper panels), and ratios of K_d^{mutant}/K_d^{WT} were determined (lower panels). **(D)** Representative SPR sensorgram showing the absence of binding of $FGF19^{\Delta C\text{-tail}}$ to KLB.

Figure S2

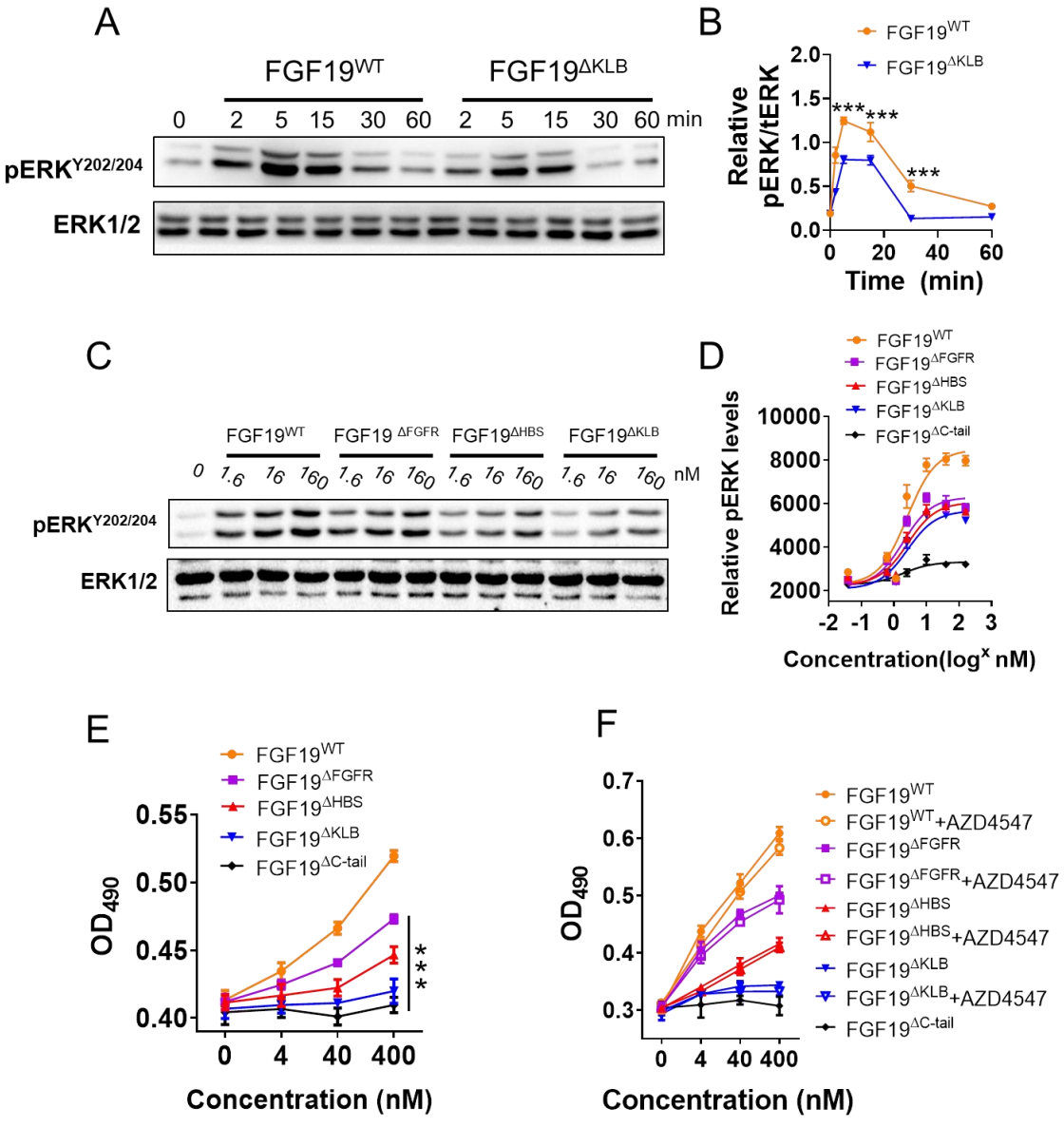

Figure S2. Cellular response induced by $FGF19^{WT}$ and its variants. (A) Immunoblots showing time-dependent activation of the MAPK pathway (ERK1/2)

by $FGF19^{WT}$ and $FGF19^{\Delta KLB}$ (16 nM) in HepG2 cells. **(B)** Quantification by densitometry of Western blot shown in (A). Data from three independent measurements are presented as mean +/- SEM; ***p<0.001 vs $FGF19^{\Delta KLB}$. **(C)** Immunoblots showing dose-dependent activation of ERK1/2 by $FGF19^{WT}$, $FGF19^{\Delta FGFR}$, $FGF19^{\Delta HBS}$ and $FGF19^{\Delta KLB}$ in H4IIE cells. **(D)** Homogeneous time-resolved fluorescence (HTRF) analysis of ERK1/2 phosphorylation in H4IIE cells induced by a range of concentrations of FGF19 and its variants. **(E)** *In vitro* proliferative activity determined by a MTT assay using H4IIE cells. **(F)** *In vitro* proliferative activity determined by a MTT assay using HepG2 cells in the absence or presence of the FGFR kinase inhibitor AZD4547. Data from three independent measurements are presented as mean +/- SEM; ***p<0.001 vs $FGF19^{WT}$.

Figure S3

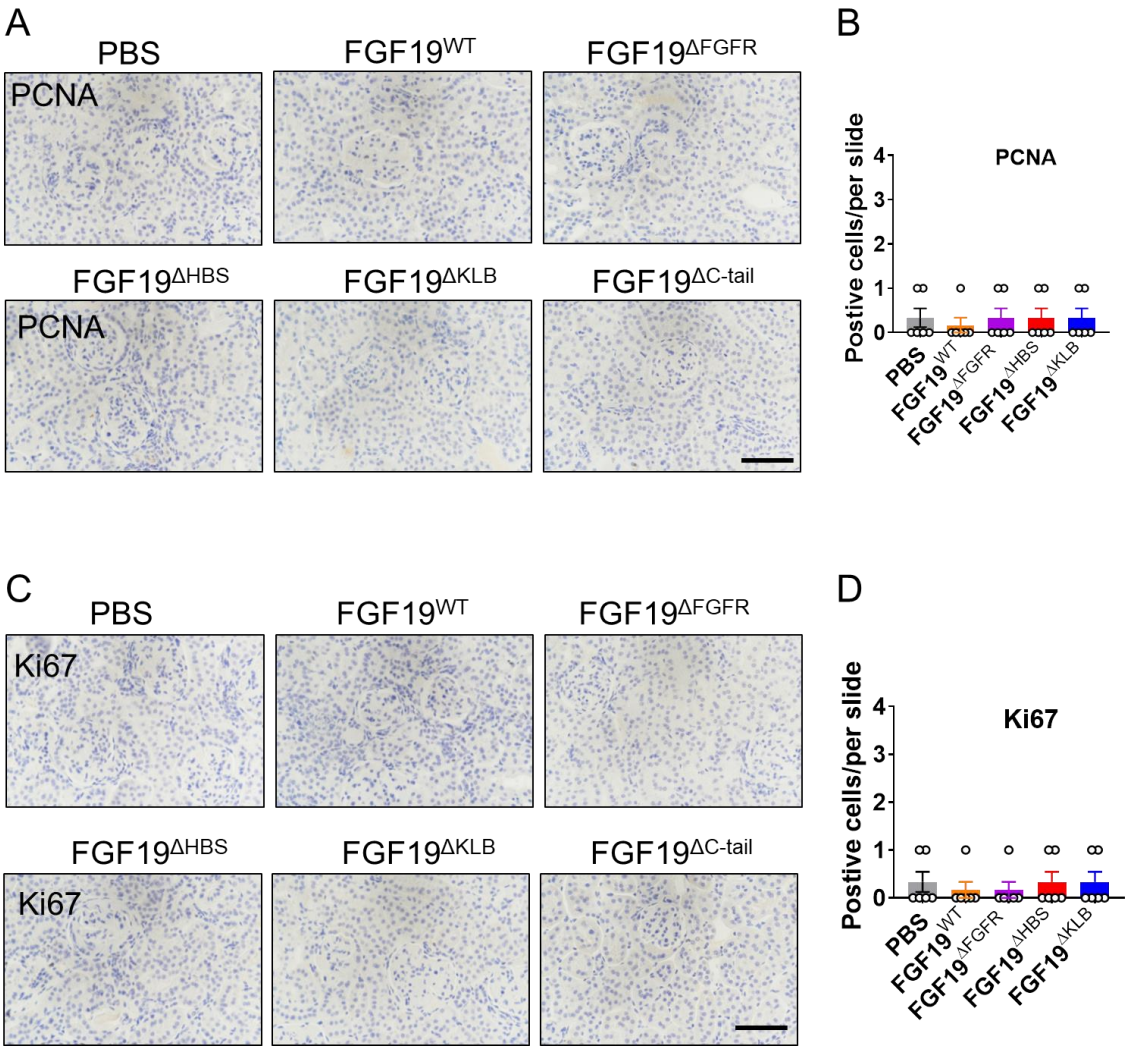

Figure S3. Mitogenic activity of FGF19^{WT} and its variants in *db/db* mouse kidney tissue. *db/db* mice were injected i.p. daily for 1 month with either FGF19^{WT}, FGF19$^{\Delta FGFR}$, FGF19$^{\Delta HBS}$, FGF19$^{\Delta KLB}$, or FGF19$^{\Delta C\text{-}tail}$ (all at 21 nmol/kg of body weight) or with PBS as a control. Panels show representative immunohistochemical staining of PCNA **(A)** and Ki67 **(C)** in kidney tissue sections and corresponding quantification by counting the number of positive dots per slide **(B,D)**. Data are presented as mean +/- SEM (n=6); scale bar, 100 μm.

Figure S4

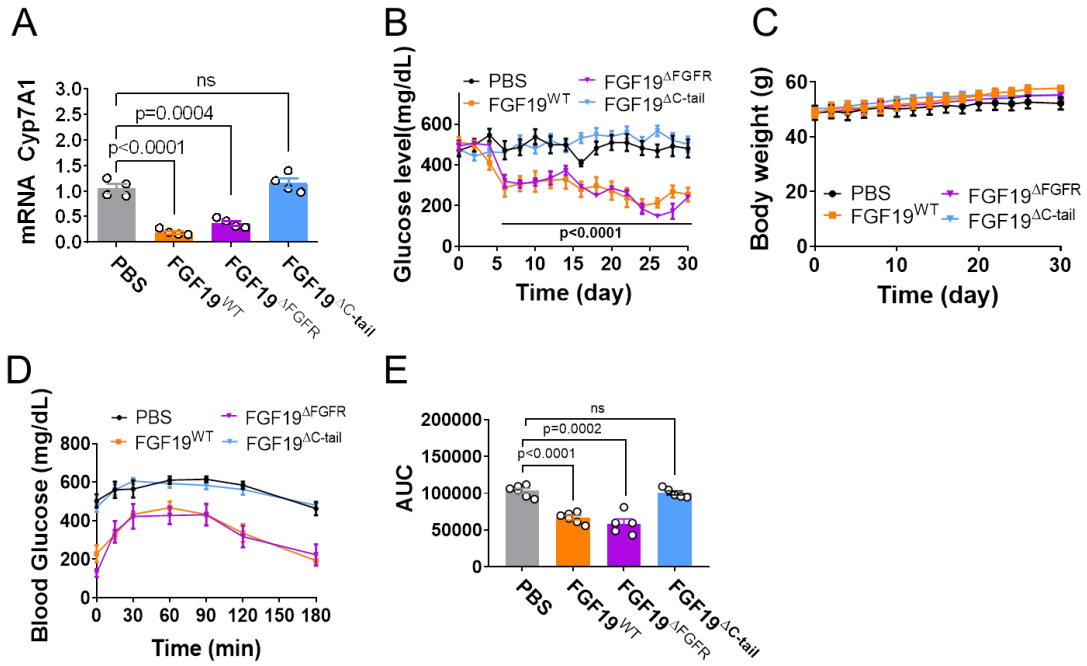

Figure S4. Bile acid and glucose homeostatic activities of FGF19$^{\Delta FGFR}$ and FGF19$^{\Delta C\text{-tail}}$. **(A)** Real-time PCR analysis of *Cyp7A1* in *db/db* mouse liver extracts 4 h after i.p. injection of FGF19^{WT}, FGF19$^{\Delta FGFR}$, or FGF19$^{\Delta C\text{-tail}}$ (all at 21 nmol/kg body weight); mice treated with PBS buffer served as controls. **(B-E)** Blood glucose (B), body weight (C), GTT (D), and integrated area under the curves (AUC) (E) for changes in blood glucose levels of ad libitum-fed *db/db* mice injected daily with FGF19^{WT}, FGF19$^{\Delta FGFR}$ or FGF19$^{\Delta C\text{-tail}}$ for 1 month; mice treated with PBS buffer served as controls. Data are presented as mean values ± SEM (n=5-6); a value of $P<0.05$ was considered statistically significant.

Figure S5

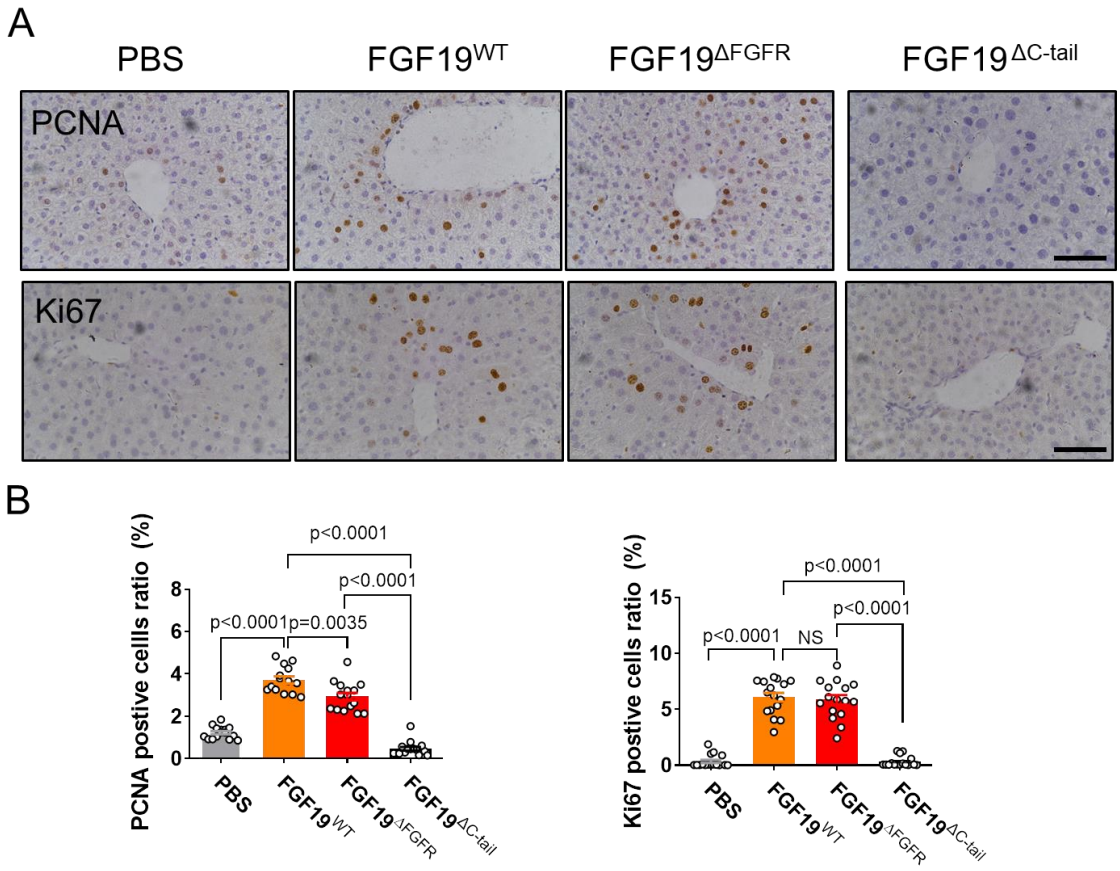

Figure S5. Mitogenic activity of FGF19$^{\Delta FGFR}$ or FGF19$^{\Delta C\text{-tail}}$ in *db/db* mouse liver tissue. **(A,B)** *db/db* mice were injected i.p. daily for 1 month with either FGF19^{WT}, FGF19$^{\Delta FGFR}$, or FGF19$^{\Delta C\text{-tail}}$ (all at 21 nmol/kg of body weight), or with PBS buffer (as a control). Panels show representative immunohistochemical staining of PCNA and Ki67 **(A)** and their corresponding quantitative analysis **(B)** done on 2-3 images of randomly selected areas from six different mice per treatment group. Data are presented as mean values ± SEM (n=15-16); a value of $p<0.05$ was considered to be statistically significant; scale bar, 100 μm.

Figure S6

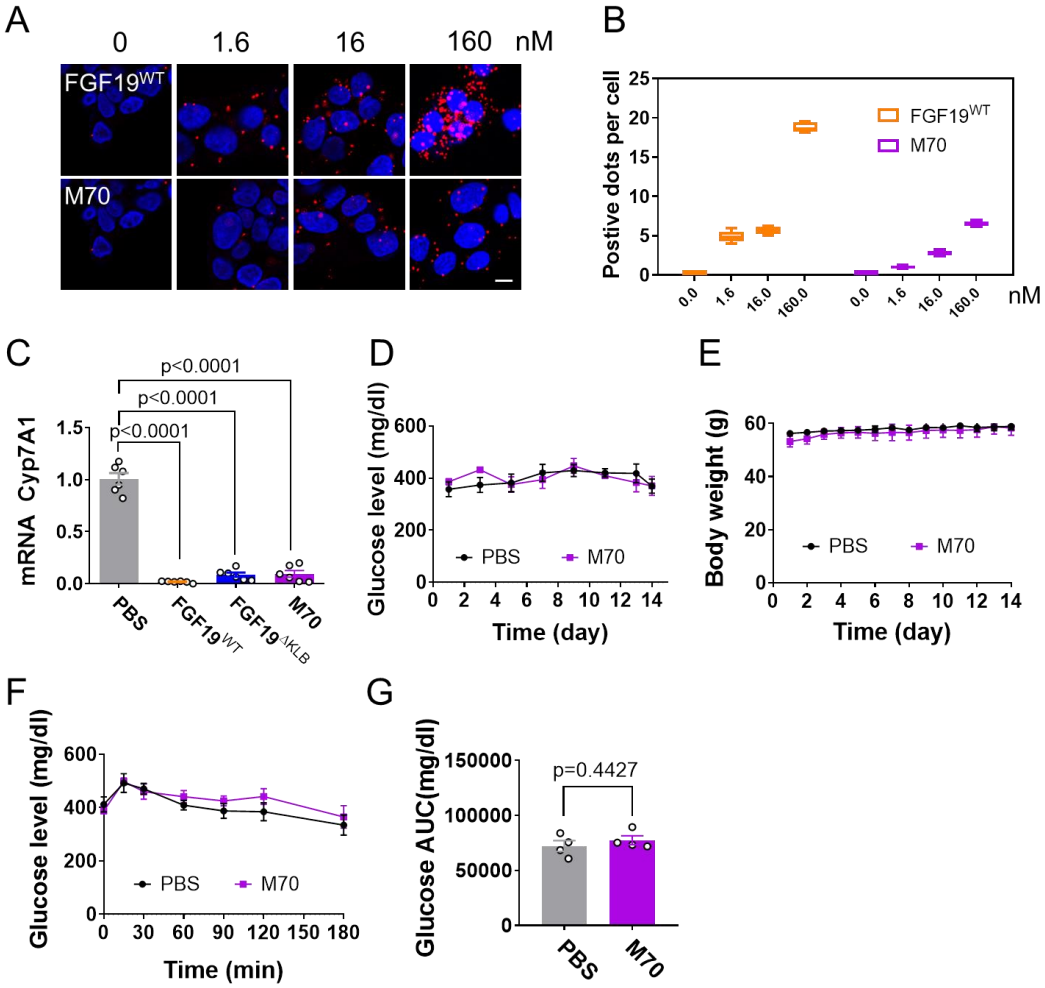

Figure S6. M70 retains BA regulation activity but lacks the glucose-lowering effect of FGF19^{WT}. **(A)** Proximity ligation assay (PLA) analysis of FGFR4 dimerization strength induced by FGF19^{WT} and M70 at 0, 1.6, 16, and 160 nM; scale bar: 10 μm. **(B)** Quantification of PLA in panel A by counting the number of positive dots per nucleus. **(C)** Real-time PCR analysis of *Cyp7A1* mRNA levels in C57BL/6J liver extracts 4 hrs after injection of FGF19^{WT}, FGF19$^{\Delta KLB}$ or M70 (all at 21 nmol/kg of body weight); mice treated with PBS served as controls. Data are presented as mean values ± SEM (n=6); a value of $p<0.05$ was considered to be

statistically significant. **(D-G)** Blood glucose (D), body weight (E), GTT (F), and integrated area under the curves (AUC) (G) for changes in blood glucose levels of ad libitum-fed *db/db* mice injected daily with M70 for 14 days; mice treated with PBS served as controls. Data are presented as mean values ± SEM (n=4).

Figure S7

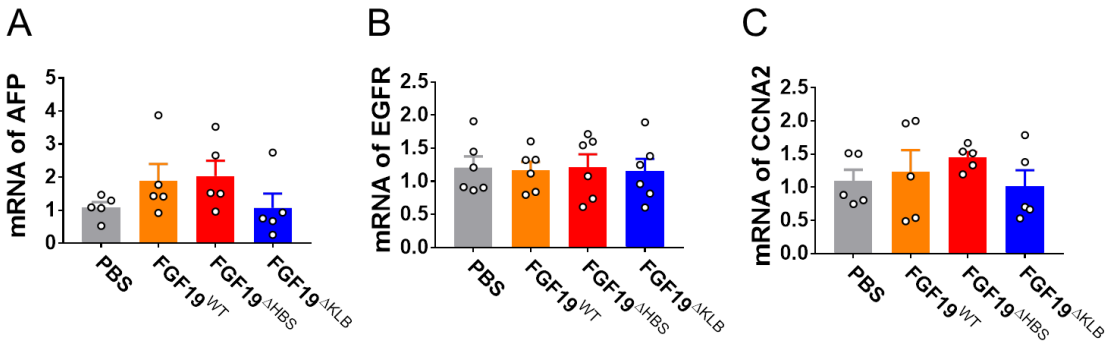

Figure S7. Cancer related biomarkers in mouse liver after 4 weeks of treatment with FGF19^{WT}, FGF19$^{\Delta HBS}$ or FGF19$^{\Delta KLB}$. Real-time PCR analysis of expression levels of AFP **(A)**, EGFR **(B)**, and CCNA2 **(C)** in livers of *db/db* mice injected i.p. with FGF19^{WT}, FGF19$^{\Delta HBS}$, or FGF19$^{\Delta KLB}$ (all at 21 nmol/kg of body weight) daily for 1 month; mice treated with PBS served as controls. Data are presented as mean values ± SEM (n=5-6).

Figure S8

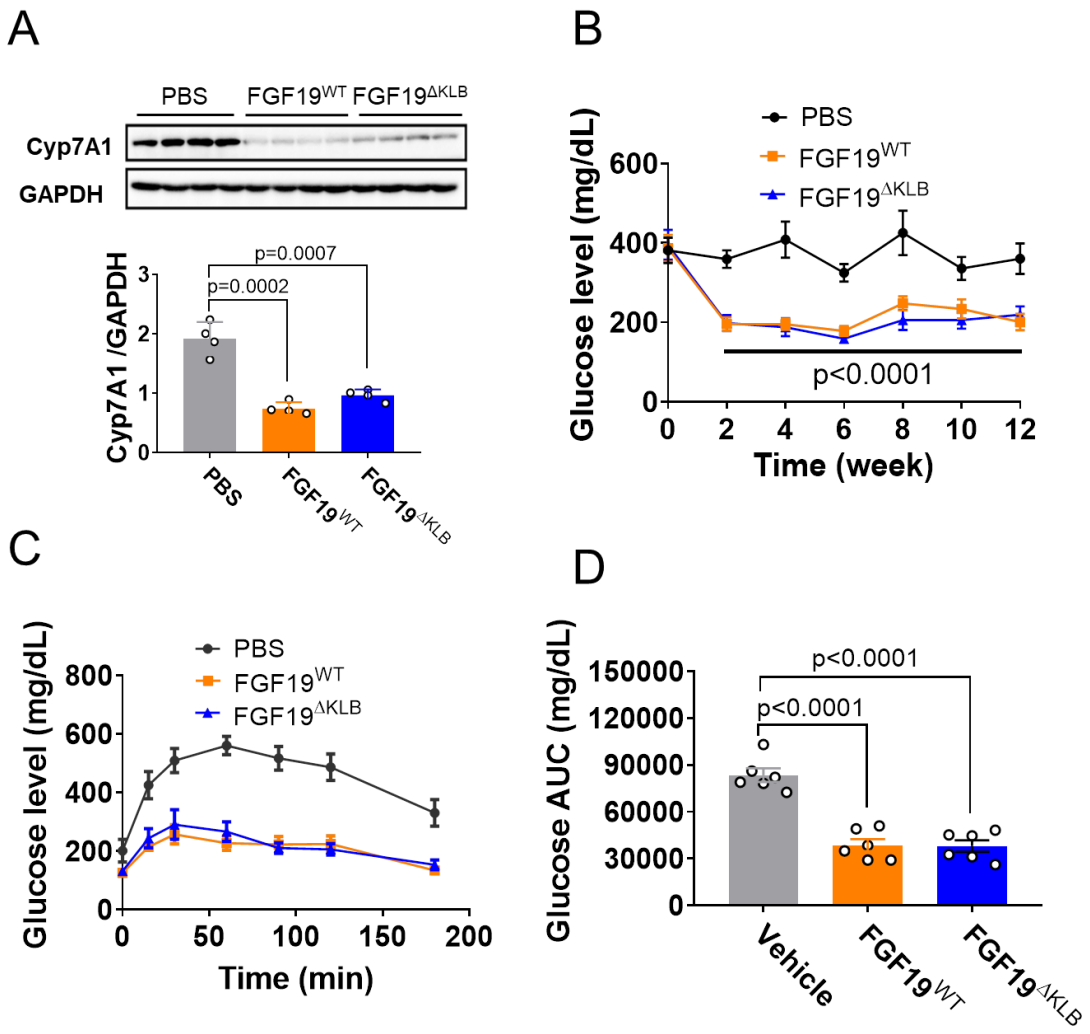

Figure S8. Bile acid and glucose regulatory activities of FGF19^{WT} and FGF19$^{\Delta KLB}$ were sustained throughout a prolonged treatment. Ad libitum-fed *db/db* mice were intraperitoneally administered with FGF19^{WT} or FGF19$^{\Delta KLB}$ (both at 21 nmol/kg of body weight) daily for 12 weeks; mice treated with PBS served as controls. (**A**) Cyp7A1 expression in excised liver as determined by western blotting (upper panel) and quantitated using ImageJ software (lower panel). (**B-D**) Blood glucose (B), a glucose tolerance test (GTT) (C) and the accompanying

integrated area under the curves (AUC) (D) for changes in blood glucose levels are shown. Data are presented as mean values ± SEM (n=6); a value of $p<0.05$ was considered to be statistically significant.

Table S1 Primers used in the RT-PCR

Gene Name	Forward (5'-3')	Reverse (5'-3')
β-actin	GGCTGTATTCCCCTCCATCG	CCAGTTGGTAACAATGCCATGT
Cyp7A1	GGGATTGCTGTGGTAGTGAGC	GGTATGGAATCAACCCGTTGTC
AFP	CTTCCCTCATCCTCCTGCTAC	ACAAACTGGGTAAAGGTGATGG
CCNA2	GCCTTCACCATTCATGTGGAT	TTGCTGCGGGTAAAGAGACAG
EGFR	GCCATCTGGGCCAAAGATACC	GTCTTCGCATGAATAGGCCAAT
Cyp8b1	CTAGGGCCTAAAGGTTCGAGT	GTAGCCGAATAAGCTCAGGAAG
Cyp27a1	CCAGGCACAGGAGAGTACG	GGGCAAGTGCAGCACATAG
Arnt2	TTATCACGTTTGTGGACCCCA	GTTGGTGCAGGTGACGTACT
Lef1	TGTTTATCCCATCACGGGTGG	CATGGAAGTGTCGCCTGACAG
Adcy1	GTCACCTTCGTGTCCTATGCC	TTCACACCAAAGAAGAGCAGG
Axin2	TGACTCTCCTTCCAGATCCCA	TGCCCACACTAGGCTGACA
Tcf7	AGCTTTCTCCACTCTACGAACA	AATCCAGAGAGATCGGGGGTC
Tgfα	GGAACCTGCCGGTTTTTGG	CACAGCGAACACCCACGTA
Prom1	GTTGAGACTGTGCCCATGAAA	GACGGGCTTGTCATAACAGGA
Nupr1	CCCTTCCCAGCAACCTCTAAA	TCTTGGTCCGACCTTTCCGA
Etv5	CGAGTTGTCGTCCTGTAGCC	GGCACAATAGTTGTAGAGGCAC
IL-6	CTGCAAGAGACTTCCATCCAG	AGTGGTATAGACAGGTCTGTTGG